

This is a “preproof” accepted article for *Mineralogical Magazine*.
This version may be subject to change during the production process.
10.1180/mgm.2025.24

Mineralogy of a cuspidine-hiortdahlite-wollastonite skarn associated with the Sierra La Vasca alkaline complex, Mexico.

Comment [SB(1)]: TE: Raise AQ for missing caption of Table 5 and 6

Roger H. Mitchell¹, Antonio Rodriguez Vega²

¹Department of Geology, Lakehead University, Thunder Bay, Ontario, Canada P7B 5E1; ²Engineering Higher School, Autonomous University of Coahuila, Nueva Rosita, San Juan de Sabina, Coahuila, Mexico

Abstract

The Tertiary Sierra La Vasca intrusive complex of the Mexican Eastern Alkaline Province consists of diverse alkaline-to-peralkaline granitoids and syenites and is a rare example of silica oversaturated peralkaline magmatism characterized by eudialyte. The intrusion of these peralkaline rocks into Cretaceous carbonate country rocks resulted in the development of a unique cuspidine, Zr-bearing cuspidine, hiortdahlite, and wollastonite exoskarn. This study is focussed on a eudialyte-bearing vein and accompanying banded exoskarn which illustrates the unusual skarn-forming metasomatic effects of Zr mobilization. The skarn consists of six mineralogically distinct zones: (1) parental Nb-poor eudialyte-bearing quartz granitoid vein; (2) a region of eudialyte pseudomorphed by intergrown Zr-sorosilicates; (3) an andradite-cuspidine-hiortdahlite-wöhlerite zone; (4) a zone of skeletal-to-prismatic cuspidine plus wollastonite which is transitional to zone (5); a coarser grained and heterogeneous zone consisting of complex intergrowths of tabular and prismatic cuspidine-hiortdahlite solid solutions, wollastonite, fluorite, apatite and rare calcite; (6) a contact calcite marble lacking any metasomatic silicates, phosphates or fluorite. Skarn formation was the result of alteration of eudialyte and separation of Si-rich hydrothermal fluids with high F/H₂O ratios from the parental Si-oversaturated peralkaline magma and subsequent infiltration of Si-Zr-REE-P-bearing fluids into the country rock carbonates. Zr was probably transported as Zr-fluoride and chloride complexes and the acidic fluids reacted with calcite to form cuspidine-hiortdahlite solid solutions and wollastonite as the principal skarn minerals. All of the Si required to form this unique skarn assemblage was derived from the hydrothermal fluids as the country rocks do not contain Si-bearing minerals. Skarn

formation is considered to have occurred at temperatures below 500°C.

Keywords: Skarn, cuspidine, hiortdahlite, eudialyte, Sierra La Vasca , Mexico

Introduction

The Sierra La Vasca alkaline complex, Mexico (25°37'43"N; 102°49'29"W) represents an occurrence of eudialyte associated with peralkaline quartz-bearing granitoids. In contrast to Si-undersaturated alkaline complexes only eight occurrences of eudialyte associated with Si-oversaturated granitoids and syenites have been previously known (Estrade *et al.* 2018; and references therein). The Sierra La Vasca complex is one of the northern members of the Mexican Eastern Alkaline Province (Fig.1; Herrera León 2019; Veira Decida *et al.* 2009) which is contiguous with the Trans-Pecos alkaline province of New Mexico and Texas (Barker, 1977). The latter also contains eudialyte-bearing rocks *i.e.* nepheline syenites at Wind Mountain (McLemore *et al.* 1996) and quartz syenites at Pajarito (McLemore , 2015). Although many skarns contain minor amounts of cuspidine (Henry, 2002; Jamveit *et al.* 1997), the Sierra La Vasca complex is apparently a unique exoskarn in consisting principally of diverse wöhlerite group minerals and wollastonite formed at the contacts of the intrusion with the country rock Cretaceous limestone. The objective of this work is to present the first detailed mineralogical description of this unique skarn and its relationship to the primary eudialyte-bearing veins.

The Sierra La Vasca complex forms a c.2 km diameter circular intrusion with an outcrop area of c. 40 km² (Fig.2). The complex has not yet been studied in any detail, although the majority of the rocks are diverse silica-rich (51-77 wt.% SiO₂; Rodriguez Vega, *unpublished*) oversaturated quartz-bearing monzonites and granitoids (Montage-Castro and Rodriguez Rodriguez 2008). All of these oversaturated rocks exhibit pronounced negative Eu anomalies in rare earth element distribution diagrams indicating significant feldspar fractionation during their genesis. Similar negative Eu anomalies are also present in the eudialyte of the veins associated with skarn formation (Rodriguez Vega; unpublished)

The north-eastern and south-western margins of the intrusion are surrounded by thin (0.2-6m) wollastonite-rich skarns. Hypersthene and quartz normative gabbro sills (Rodriguez Vega; *unpublished*) occur adjacent to the north-western margin (Fig.2). The wollastonite skarns have been previously investigated as potential sources of industrial minerals by Diaz-Martinez *et al.* (2022). Monumental Minerals Inc., undertook a limited, and now abandoned, exploration project for wollastonite and rare earth elements at the eastern margin of the complex (*Monument Energy*

News Releases of May 2022, August 2023).

Analytical Methods

Polished thin sections were examined by optical and back-scattered electron petrographic methods. Compositions of the phases present were determined by *quantitative* energy dispersive X-ray spectrometry using a Hitachi FE-SU70 scanning electron microscope equipped with the Oxford Instruments AZtec software package. The electron accelerating voltage was 20 kV and the beam current 300 pA. Standards used were: wollastonite (Si,Ca); corundum (Al); jadeite (Na,Al); BaF₂ (Ba, F); Mn-hortnonolite (Mg, Fe Si, Mn); synthetic rare earth element phosphates (La, Ce, Pr, Nd, Sm, P); SrTiO₃ (Sr, Ti); ThNb₄O₁₂ (Th, Nb); ilmenite (Ti, Fe) and Zr metal. The rastered beam over an area of 15 x 15 microns and low beam currents (300pA) employed for quantitative X-ray energy dispersive spectrometric analysis permitted accurate and reproducible analysis of small crystals (< 50 microns) in a variety of hosts without excitation of the latter.

Mineralogical Character of the Skarn Zones

The wollastonite skarns are developed adjacent to complex magmatic veins of eudialyte granitoids. Figure 3a illustrates the macroscopic complexity of the relationships of the skarn zone to the eudialyte bearing veins and the limestone country rocks. Each vein is surrounded skarn zones of differing width and mineralogy. This study is focussed on a representative small eudialyte-bearing vein and accompanying exoskarn (Fig.3b) which illustrates the unusual skarn-forming and metasomatic effects of Zr , REE and Nb mobilization.

The material investigated (Fig. 4) consists of a ~2 cm eudialyte-rich vein, adjacent skarn (~6 cm) and country rock marble. Although small, this vein material is a microcosm of the more complex and extensive skarn assemblages associated with the eudialyte granitoids. The, skarn is considered to consist of six mineralogically distinctive zones; (1) parental eudialyte vein ; (2) a region of pseudomorphed eudialyte; (3) a garnet-cuspidine,hiortdahlite,wöhlerite zone; (4) a zone of fine grained wollastonite and skeletal-to-prismatic cuspidine which is transitional to zone (5) which is coarser grained and heterogeneous, consisting of complex intergrowths of wollastonite, diopside, Zr-bearing cuspidine-and hiortdahlite prisms, fluorite, apatite and calcite; (6) the contact calcite marble which lacks any metasomatic silicates, phosphates or fluorite. Skarn zones 2-5 account approximately for 11, 22, 11, and 56 % of the skarn, respectively

Zone 1: Petrography of the Eudialyte Granitoid

The eudialyte granitoid consists of pale red euhedral-to-subhedral (0.5-2 mm) eudialyte phenocrysts which have been concentrated by flow differentiation set in a matrix of poikilitic aegirine with interstitial quartz, albite, and potassium feldspar. The eudialyte crystals are colourless and homogeneous in thin section in plane polarized light and exhibit heterogeneous anisotropic first order interference colours (Fig.5). The latter are interpreted to result from incipient alteration of the eudialyte (See below). In back-scattered electron (BSE) images the majority of the crystals do not show any compositional zoning, although a few have irregular thin mantles with higher BSE contrast, reflecting minor increased Nb content (see below). The eudialyte contains rare inclusions of wöhlerite and Ca-catapleiite.

The eudialyte phenocrysts are set in a groundmass of poikilitic green aegirine of uniform colour and composition ($Ae_{73}Hd_{23}Di_4$). The late-stage mesostasis to the aegirine is composed principally of irregular intergrowths (Fig. 6A) of albite ($Ab_{93}Or_7$) and Fe-bearing potassium feldspar ($Or_{96.2}Fe-Or_{3.8}$) with later-crystallizing quartz, poikilitic britholite (Fig. 6B), Ca-catapleiite prisms, rare wöhlerite and a thorongummite-like mineral.

Petrography of Zone 2

Adjacent to the eudialyte granitoid vein, Zone 2 consists primarily of fine grained optically unresolvable material pseudomorphing eudialyte. Back-scattered electron images (Figure. 7a) illustrates a well-defined transition from fresh eudialyte to a complex, heterogeneous and fine grained intergrowth of cuspidine-hiortdahlite solid solution, diopside and Mn-bearing wollastonite.(Fig. 7b).

Petrography of Zone 3

Zone 3 is essentially optically unresolvable in thin sections with isotropic regions (Fig.4) reflecting the dominance of Zr-bearing andradite (Fig. 8a). BSE imagery shows the additional presence of a heterogeneous assemblage of Zr-bearing cuspidine-hiortdahlite solid solution, wöhlerite, diopside, and wollastonite with trace chalcopyrite, sphalerite and a thorongummite-like mineral (Fig. 8b).

Petrography of Zones 4 and 5

These zones form the major part of the skarn and are characterised by cuspidine, Zr-bearing cuspidine and hiortdahlite set in a wollastonite matrix. Zones 4 and 5 differ primarily in

terms of their texture. The finer grained zone 4 consists primarily of wollastonite plus skeletal-to-prismatic cuspidine (Fig.9a) with minor apatite. This zone is transitional to the coarser grained heterogeneous zone 5 consisting of complexly intergrown wollastonite, diopside, cuspidine and Zr-bearing cuspidine prisms, fluorite, apatite and rare calcite (Figs. 9b-d). Complexly zoned and resorbed cuspidine prisms (Fig. 10a,b) are characteristic of this zone and concentrated in regions near to the contact with the country rock marble.

Petrography of Zone 6

The country rock marble consists only of a fine grained granular polygonal calcite. The contact of zone 5 with the marble is well defined (Fig. 9d).

Mineral Compositions

Eudialyte

The eudialyte exhibits only minor compositional variation and the majority of crystals are uniform with respect to all major elements. Minor Nb-enrichment of up to 1 wt.% Nb₂O₅ is evident only in some marginal discontinuous partial overgrowths. Representative compositions of eudialyte are given in Table 1 which shows that the mineral is poor in REE, Mn, Nb and represents a solid solution between eudialyte (75-82 mol.%) and kentbrooksitite (13-18 mol.%) with minor alluaivite (3-9 mol.%). The La Vasca eudialyte is not of unusual composition compared to other early magmatic eudialyte found in both silica oversaturated and undersaturated alkaline complexes (Fig. 11). The eudialyte have total oxide compositions ranging from 96.4 to 97.7 wt.% for major elements for the elements analysed. Such compositions are not unusual for eudialyte occurring in diverse parageneses (Schilling et al. 2011; Liferovich and Mitchell 2006, Chakrabarty et al. 2018; van de Ven et al. 2019).

The heterogeneous optical anisotropism shown by the La Vasca eudialyte (Fig.5b) is not evident in the BSE imagery, or major element compositional data, and we are confident that it does not represent significant Na loss due to electron beam damage under our analytical conditions. An explanation of the anisotropism, which might represent incipient Na-loss (Mikhailova et al. 2022) or variation in vacancies, O, OH⁻, H₂O, CO₃²⁻ content is beyond the scope of this paper.

Hiortdahlite - cuspidine solid solutions

Minerals belonging to the wöhlerite group (Dal Bo et al. 2022) are abundant in zones 2-5

of the skarn. Wöhlerite $[\text{Na}_2\text{Ca}_4\text{ZrNb}(\text{Si}_2\text{O}_7)_2\text{O}_3\text{F}]$; Table 2] is relatively uncommon in this skarn and the majority of the group present are Nb-poor minerals which represent members of a solid solution series between cuspidine $[\text{Ca}_8(\text{Si}_2\text{O}_7)_2\text{F}_4]$ and hiortdahlite $[\text{Na}_2\text{Ca}_4(\text{Ca}_{0.5}\text{Zr}_{0.5})\text{Zr}(\text{Si}_2\text{O}_7)_2\text{OF}_3]$. These minerals occur as alteration products of eudialyte (zone 2) and as primary metasomatic phases formed in association with wollastonite (zones 3-5).

Tables 2 and 3 give representative compositions of cuspidine, Zr-bearing cuspidine and hiortdahlite. Paragenetic relationships between these minerals are complex although it is evident that cuspidine is the principal pseudomorphing phase of eudialyte, and as early-forming prismatic crystals in the skarn (Fig.9a). Prismatic cuspidine and Zr-bearing cuspidine crystallize together with abundant large plates of hiortdahlite in a wollastonite matrix in skarn zones 4-5 (Fig.9). The Zr-bearing cuspidine exhibits significant irregular compositional zoning with respect to Zr-contents which extend towards the composition of hiortdahlite (Fig. 12), indicating the existence of a previously unrecognized solid solution series between cuspidine and hiortdahlite. Niobium contents are all low (< 1 wt.% Nb_2O_5). The compositions of hiortdahlite in the La Vasca skarn are identical with those of this mineral from the type locality (Table 2).

Britholite

Britholite is a common trace accessory mineral in the eudialyte granitoid vein as a late stage complexly zoned poikilitic phase (Fig .6b) and as small (< 20 micron) ovoid crystals in zones 3 and 4, and with rarer occurrences in zone 5 of the skarn. The britholite is notable in that it contains significant amounts of Y_2O_3 (1.4-5.9 wt.%; Table 4), although it never approaches the composition of britholite-(Y). Composite asymmetric fluorine ($\text{K}\alpha$)–Ce ($\text{M}\alpha$) low energy peaks at 0.677 and 0.884 Kev were not observed in the X-ray spectra of britholite, suggesting that F contents are very low or below the limit of detection in the presence of abundant Ce. Thus, the mineral at La Vasca is considered to be britholite-(Ce) i.e. $[\text{Ca,REE,Y}]_5(\text{SiO}_4, \text{PO}_4)_3\text{OH}$.

Other Major Silicate Skarn-forming Minerals

Wollastonite (CaSiO_3) is the most abundant late-forming Zr-free mineral in skarns zones 3-5, and has near stoichiometric compositions with only minor amounts MnO (0.2-1.0 wt.%). Garnet dominates zone 3 and ranges in composition from andradite to Zr-bearing andradite (Table 4). Diopside compositions in skarn zones 3-5 are near the ideal end member $\text{CaMgSi}_2\text{O}_6$ with very minor compositional variation with respect to FeO_T (2.2- 3/1 wt.%). Recalculation of the compositions on stoichiometric basis suggests minor amounts of a fassaite component in

some crystals (Table 4).

Other skarn-forming Minerals

Calcite, Ca-catapleiite, fluorite, apatite, rare zircon (1.2-1.5 Wt.% HfO₂) and pectolite replacing wollastonite, are all of near-stoichiometric composition. Ca-catapleiite (Table 4) contains minor FeO (0.17-0.58 wt.%) and Na₂O (0.62-0.91 wt.%). Apatite is F-bearing (2.9 wt.%), lacks Sr (<0.3 wt.% SrO) and is poor in Si and REE(1.5 SiO₂; 1.3 Ce₂O₃ wt.%). Other trace minerals are a thorumite-like mineral (46.6 ThO₂; 20.58 SiO₂; 9.70 CaO ; 8.2 REE₂O₃ wt.%), and very rare Ca-Nb pyrochlore .

Discussion

The Sierra La Vasca skarn is unique relative to common exometasomatic skarns associated with diverse igneous intrusions in that it is dominated by Ca-Zr-F-bearing sorosilicates belonging to the wöhlerite structural group. Although, the skarn contains significant amounts of wollastonite it differs from the typical skarns formed from impure limestone country rocks (Meinert et al. 2005) as it does not contain gehlenite, åkermanite, monticellite, grossular, larnite or spurrite. Such Zr-bearing sorosilicate-wollastonite dominated skarns were not recognized in the review of skarn deposits by Meinert et al. (2005).

With the exception of calcium, the components of the minerals forming the skarn were derived from the eudialyte-bearing peralkaline granitoid vein by late stage fluids developed during a magmatic to hydrothermal transition. This process is well-known (Meinert et al. 2005) and is responsible for the formation of most exometasomatic skarns. In the case of the La Vasca skarn the presence of fluorite and abundant F-bearing sorosilicates together with the paucity of hydrous minerals implies that fluids emanating from the eudialyte vein must contain considerable fluorine and have low water contents. Thus, F/H₂O ratios must be very high. In addition, the eudialyte occurring in zone 1 contains chlorine and its decomposition must add this to the skarn-forming fluids. However, the absence of Cl-bearing minerals suggests that the Cl contents of these fluids must have been low relative to the fluorine content and that F/Cl ratios must have been high . .

At Sierra La Vasca, transport of the F-rich fluids into the country rock limestone resulted in fluid-infiltrated reaction zones and formation of a banded exoskarn. Temperatures of the reactions were undoubtedly low and certainly, because of the presence of fluorine and eudialyte

crystallization, probably at temperatures well below those of the water-bearing “granitoid (QZ₃₇Ab₃₄Or₂₉) minimum” melting temperature of 750°C at 1kb (Hamilton and Mackenzie 1965), as represented by the assemblage of quartz+K-feldspar+albite in the eudialyte-bearing veins. In this respect, Manning (1981) has shown that with increasing F content the position of the quartz-alkali feldspar boundary moves away from the quartz apex of this ternary system and with 4 wt.% F the minimum melting composition is QZ₁₅Ab₅₈Or₂₇ at 630°C. Manning (1981) also notes that minimum melting temperatures as low as 550°C at 1 kb are possible for some bulk compositions (QZ₂₅Ab₅₅Or₃₀ + 4 wt.% F). Unfortunately, experimental studies of eudialyte granitoid compositions have not been undertaken. With respect to this skarn, temperatures of <450°C have been proposed by Mitchell and Liferovich (2006) for alteration of eudialyte in peralkaline nepheline syenites and Mikailova et al. (2022) have demonstrated eudialyte can be replaced at temperatures as low as 230° C in acidic H₂O-NaCl solutions with pH 5.6-1.8. It is suggested, on the basis of the above, that the emplacement temperature of the veins must have been on the order of 600°C and that fluids emanating from these veins during the magmatic to hydrothermal transition were initially at this, or lower, temperatures. These fluids caused subsolidus alteration of the eudialyte and permeated the limestone country rock as Zr-anion bearing fluids.

Petrographic studies of the Sierra La Vasca skarn suggest formation by kinetic diffusional processes as the skarn is mineralogically and compositionally zoned. The constituent minerals in each of the zones are distributed heterogeneously and form apparently non-equilibrium assemblages. The mineralogical zoning indicates that different elements were transported at different distances from the eudialyte source vein into the country rock limestone. Figure 13 illustrates this differential transport for major components of the skarn. Importantly, Zr and Si have been transported together and have formed the cuspidine-hiortdahlite solid solutions throughout the skarn. However, these minerals differ with respect to their habit as they form: (1) fine grained anhedral crystals replacing eudialyte (Fig. 7b); (2) long skeletal-to-prismatic crystals in zone 4 at the contact with zone 3 (Fig.9a); (3) blocky tabular crystals in zone 5 (Fig.9c); and (4) large skeletal zoned partially-resorbed crystals in zone 5 at the contact with the country rock (Fig.10a,b).. The differing habits in zones 4 and 5 suggest rapid non-equilibrium crystal growth prior to the formation of the wollastonite groundmass.

Of note is that andradite garnet is preferentially formed adjacent to the vein (zone 3) and

the Fe depletion of the skarn forming fluids is such that pyroxenes in zone 4 and 5 are essentially pure diopside. Rare earth elements are rapidly depleted in zone 3 and britholite crystallization ceases resulting in fluorapatite becoming the principal phosphate in zones 4 and 5.

Of particular significance is the observation that the country rock limestone is devoid of quartz or other silicates (Fig.10d). Thus, wollastonite cannot have been formed simply from siliceous limestone at conditions in the P-T ranges ($>600^{\circ}\text{C}$; >5 kb) of the solid state calcite + quartz univariant reaction curve determined by Harker and Tuttle (1956). Hence, the Si required to form the cuspidine-hiortdahlite solid solutions and wollastonite must have been entirely derived from the low temperature fluids emanating from the eudialyte granitoid vein. The solubility of Si in hydrothermal solutions has been extensively investigated at low temperatures (350 - 600°C) and pressures ranging up to 175 MPa (Kennedy 1950; Anderson and Burnham 1965), and it is clear that significant amounts, e.g. 0.12 wt.% SiO_2 at 50 MPa at 370°C are possible, and could result in the formation of the silicate assemblage in this skarn.

Although there is an absence of H_2O -bearing minerals in the skarn, the fluids which from which the Zr-bearing sorosilicates crystallized undoubtedly contained diverse H_2O - and OH^- bearing Zr-anion complexes. The existence of such F-bearing complexes has been investigated by Migdisov et al. (2011) and Loges et al. (2022) who have shown these to consist of $\text{ZrF}(\text{OH})_3^{\ominus}$, $\text{ZF}_2(\text{OH})_2^{\ominus}$, and $[\text{Zr}(\text{F},\text{OH})_4.2\text{H}_2\text{O}]^{\ominus}$. Filimonova et al. have also demonstrated the existence of $\text{ZrCl}_3(\text{OH})_2^-$ and $\text{ZrCl}_5(\text{H}_2\text{O})^-$ complexes at low temperatures (320 - 480°C) in HCl - H_2O hydrothermal experiments at 2 kb. The actual metasomatic transfer of Zr into skarns by fluid infiltration to form zirconolite or baddelyite has been documented by Guo et al. (2024) and Zhao et al. (2016).

Calcite is typically absent, or rare, in the skarn and its absence undoubtedly is related to its dissolution by the acidic hydrothermal Si-Zr-fluids infiltrating the country rock carbonate along grain boundaries with accompanying reaction to form cuspidine, Zr-bearing cuspidine and-hiortdahlite prior to wollastonite; the latter forming after Zr-depletion.

Although there are many studies of cuspidine formation at high temperatures there are few experimental investigations of its formation or phase relationships in hydrothermal systems. None of these contained Zr, and we are not aware of any experimental studies of hiortdahlite formation. Cuspidine was initially synthesized by Van Valkenburg and Rynder (1958) at temperatures of $<500^{\circ}\text{C}$ at 138MPa). A recent study of cuspidine formation in the system CaO -

SiO₂.nH₂O by Gineika and Baltakys (2023) demonstrated the rapid formation of cuspidine at low temperature and pressure *e.g.* with 12 hours at 130°C and 4 hours at 150-200°C. In the [CaO-(Al-bearing silica gel)-CaF₂-H₂O] system, cuspidine formed within four hours and was the main compound in the synthesis products. From these studies it is suggested that the cuspidine-hiortdahlite solid solution series probably can form rapidly in skarns at temperatures ranging from 200-500°C. Pressures prevailing are not known but can be expected to be < 0.5 kb on the basis of the regional geology.

In conclusion, textural, petrographic and experimental evidence suggests that the Sierra La Vasca cuspidine-hiortdahlite-wollastonite skarn formed rapidly and at relatively low temperatures by the infiltration of acidic Si-F-Zr-bearing hydrothermal fluids, derived from a eudialyte quartz granitoid into a pure calcite limestone. In contrast to common exoskarns (Meinert et al. 2005), the La Vasca skarn is dominated by sorosilicates and wollastonite as a consequence of the relative paucity of Al, Na, Ti, and Mg in the parental fluids. Although the vein investigated is small, it is part of a larger anastomosing suite of veins, and the conclusions of this study are relevant to the genesis of the contact metasomatic aureole of the complex as a whole. This skarn also shows clearly that under F-rich conditions Zr and Nb are mobile elements.

Acknowledgements .

This contribution to the Edward Grew Volume is in recognition of his outstanding record as a mineralogist and his significant contributions to the Mineralogical Society of Great Britain and Ireland as a long term Associate Editor for the Mineralogical Magazine. This study of the La Vasca skarn was supported by Lakehead University, the Universidad Autónoma de Coahuila and Almaz Petrology. We thank Michael Anenburg and Darrell Henry for useful reviews of this contribution.

References

- Anderson G.M. and Burnham C.W. (1954) The solubility of quartz in super-critical water. *American Journal of Science*, **263**, 494-511.
- Barker D.S. (1977) Northern Trans-Pecos magmatic province: introduction and comparison with the Kenya Rift. *Geological Society of America Bulletin*, **88**, 1421-1427.

- Borst A.M. Friis, H., Anderson T., Nielsen, T.F.D., Waight T.E. and Smit M.A. (2019) Zirconosilicates in the kakortokites of the Ilímaussaq complex, South Greenland: Implications for fluid evolution and high-field strength and rare-earth element mineralization in apgaitic systems. *Mineralogical Magazine*, **80**, 5-30.
- Chakrabarty A., Mitchell R.H., Ren M., Pal S., Pal.S and Sen K. (2018) Nb-Zr-REE-re-mobilization and implications for transitional apgaitic rock formation: Insights from the Sushina Hill Complex, India. *Journal of Petrology* , 59,1899-1938.
- Diaz-Martinez R., Elias-Ortiz N.P. and Rodriguez-Vega A. (2022) Wollastonita asociada al magmatismo alcalino en la sierra La Vasca, Coahuila. Pp. 203-215 in : *Metalurgia, Geologia y Minas: Avances para un Futura Sustentable* Alvaroado-Macias G., Rosales-Marin G., Andrade-Martinez J. and Navio-Gomez D. editors). Universidad Autónoma de San Luis Potosi, Mexico (ISBN 978-607-535-293-0) .
- Dal Bo F., Friis H. and Mills S.J. (2022) Nomenclature of the wöhlerite group minerals. *Mineralogical Magazine*, **86**, 661-676.
- Droop G.T.R. (1987) A general equation for estimating Fe³⁺ concentrations in ferromagnesian silicates and oxides from microprobe analyses using stoichiometric criteria. *Mineralogical Magazine*, **51**, 431-435.
- Estrade G., Salvi S. And Béziat D. (2018) Crystallization and destabilisation of eudialyte group minerals in peralkaline granite and pegmatite: case study from the Ambohimirahavavy complex, Madagascar. *Mineralogical Magazine*, **82**, 375-399.
- Filimonova O.N., Trigub A.L., Shikina N.D., Nickolsy M.S. and Tagirov B.R (2023). The state of Zr and Hf in chloride hydrothermal fluids from in situ X-ray absorption spectroscopy. *Chemical Geology*, 641 (2023) 121787.
- Gineika A. and Baltakys K. (2023) The effect of hydrothermal treatment conditions and silica source on the formation of cuspidine. *Journal of Thermal Analysis and Calorimetry*, **198**, 3965-3974
- Guo Q., Guo S., Yang Y., Mao Q., Yuan J., Wu S., Liu X. and Sein K. (2024) Multiple growth of zirconolite in marble (Mogok metamorphic belt, Myanmar): Evidence for episodes of fluid metasomatism and Zr-Ti-U mineralization in metacarbonate systems. *European Journal of Mineralogy*, **36**, 11-29.
- Hamilton D. L. and Mackenzie W.S. (1965) Phase equilibria in the system NaAlSiO₄ - KAlSiO₄

-SiO₂ . *Mineralogical Magazine*, **34**, 214-231.

- Harker R.I, and Tuttle O.F. (1956) Experimental data on the P_{CO_2} - T curve for the reaction : calcite + quartz = wollastonite + carbon dioxide. *American Journal of Science*, **254**, 239-256.
- Henry D.A. (2002) Cuspidine-bearing skarn from Chesney Vale, Victoria. *Australian Journal of Earth Sciences*, **46**, 251-260.
- Jamveit B., Dahlgren S. A. and Austrheim H. (1997) High grade contact metamorphism of calcareous rocks from the Oslo Rift. *American Mineralogist*, **82**, 1241-1254.
- Kennedy G.C. (1950) A portion of the system silica-water. *Economic Geology*, **45**, 629-653.
- Herrera León M.A. (2019) Petrografía y Geoquímica del Intrusivo Colorado, Cinturón Candela-Monclova Provincia, Alcalina Oriental Mexicana. Thesis Universidad Autónoma de Nuevo León, Linares, Nuevo León, Mexico .
- Loges A., Manni, M., Louvel M., Wilke M., Jahn S., Welter, E., Borchert M., Qiao S., Klemme S., Keller B.G. and John T. (2024) Complexation of Zr and Hf in fluoride-rich hydrothermal aqueous fluids and its significance for high field strength element fractionation. *Geochimica et Cosmochimica Acta*, **366**, 167-181. (doi.org/10.1016/j.gca.2023.12.013)
- Manning D.A.C. (1981) The effect of fluorine on liquidus phase relationships in the system Qz-Ab-Or with excess water at 1 kb. *Contributions to Mineralogy and Petrology*, **76**, 206-215.
- Meinert L.D., Dipple G.M. and Nicolescu D. (2005) *World Skarn Deposits* in: 100 Anniversary Volume ,(Hedquist, J.W., Thompson J.F.H., Goldfarb, R.J. and Richards , J.P. editors), Society of Economic Geology Publishing Company (doi.org/10.5382/AV100.11)
- McLemore V.T. (2015) Rare Earth Elements (REE) Deposits in New Mexico: Update. *New Mexico Geology*, **37**, 59-69.
- McLemore V.T., Lueth V.W. and Pease T.C. (1996) Petrology and mineral resources of the Wind Mountain laccolith, Cornudas Mountains, New Mexico and Texas. *Canadian Mineralogist*, **34**, 335-347.
- Migdisov A.A., Williams-Jones A.E., van Hinsberg V. and Salvi S. (2011) An experimental study of the solubility of baddelyite (ZrO₂) in fluoride-bearing solutions at elevated temperature. *Geochimica et Cosmochimica Acta*, **75**,746-7434.

- Mikhailova J.A., Pakhomovsky Y.A., Kalashnikova G.O. and Aksenov S.H. (2022) Dissolution of the eudialyte group minerals: Experimental modelling of natural processes. *Minerals*, **12**, 1460 (doi.org/10.3390/min12111460).
- Mitchell R.H. and Liferovich R.P. (2006) Subsolidus deuteric/hydrothermal alteration of eudialyte in lujavrite from the Pilansberg alkaline complex, South Africa. *Lithos*, **91**, 352-372.
- Montañez Castro A. and Rodriguez-Rodriguez J.S. (2008) Carta Geológico-Minera San Miguel H13-D67, Coahuila, Escala 1:50 000 . Pachuca, Hidalgo, México: *Servicio Geológico Mexicana*.
- Pfaff K., Wenzel T., Schilling J. and Markl G. (2010) A fast and easy to use approach to formula calculation for eudialyte group minerals. *Neues Jahrbuch für Mineralogie A*, **187**, 69-81.
- Schilling J., Wu F-Y., McCammon C., Wenzel T., Marks M.A.W., Pfaff K, Jacob D.E. and Markl G. (2011). The compositional variability of eudialyte group p minerals. *Mineralogical Magazine*, **75** 87-115.
- van de Ven M.A.J., Borst A.M., Davies G.R., Hunt E.J. and Finch A.A. (2019). Hydrothermal alteration of eudialyte hosted critical metal deposits: Fluid source and implications for deposit grade. *Minerals*, **9**, 422 (doi/org: 10.3390/min9070422)
- Van Valkenburg A. and Rynders G.F (1958) Synthetic cuspidine. *American Mineralogist*, **43**, 1195-1202
- Veira-Decida F., Ramirez-Fernandez J.A., Velazco-Tapia F. and Orozco-Esquivel M.T. (2009) Relaciones petrogenéticas del magmatismo en la Provincia Alcalina Oriental Mexicana . *Ciencia Universidad Autónoma de Nuevo León*, **12**, 42-49
- Zhao W-W., Zhou, M-F. and Chen W-T. (2016) Growth of hydrothermal baddelyite and zircon in different stages of skarnitization. *American Mineralogist*, **101**, 2689-2700.

List of Figures

Figure 1. Location of the Sierra La Vasca complex with respect to the volcanic provinces of Mexico (after Herrera León, 2019 and Viera-Decida *et al.* 2009).

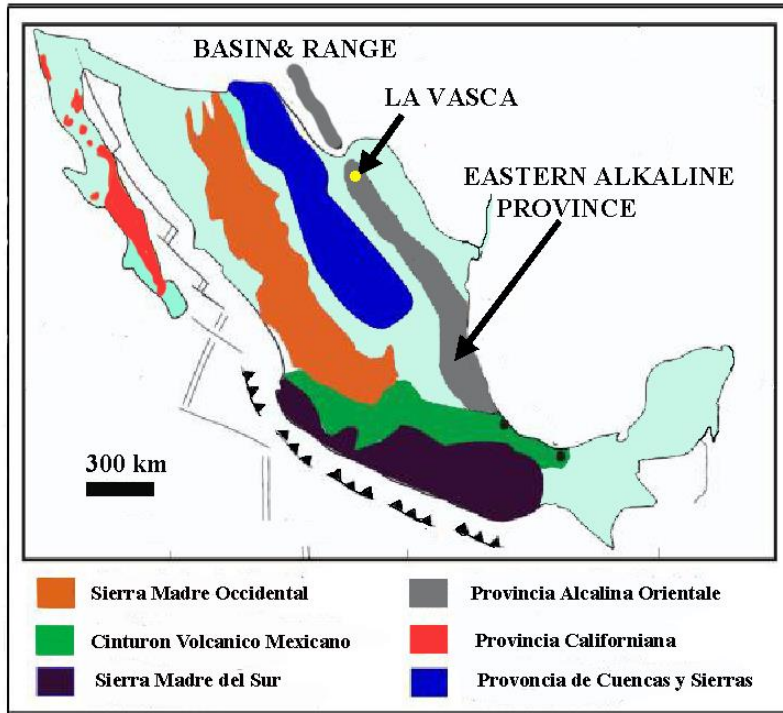


Figure 2. The Sierra La Vasca complex.(A) Satellite image (Google Earth) illustrating the topographic character; (B) Geological map (after Montañez Castro and Rodriguez Rodriguez, 2008), The yellow rectangles in the south eastern part of the complex indicate areas of high wollastonite content, whereas those in the north-west encompass a region of gabbro sills.

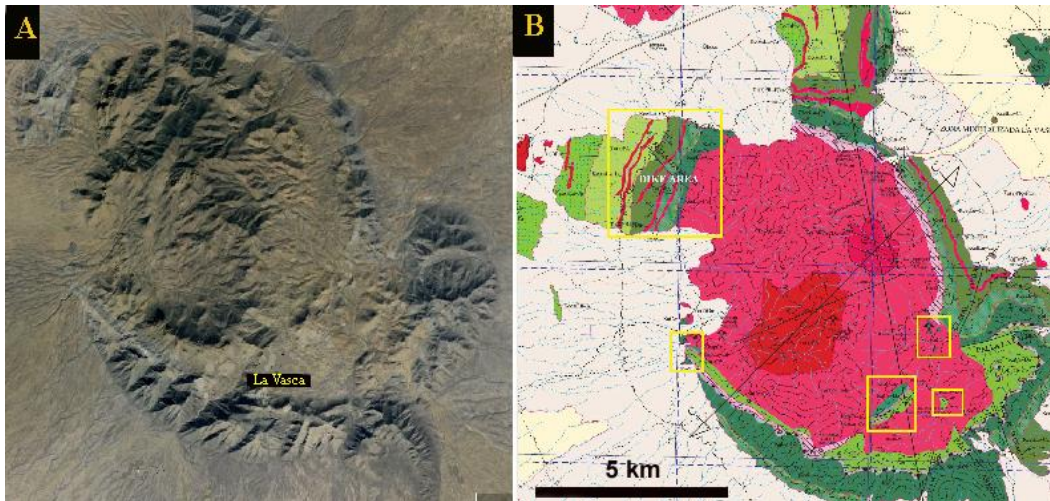
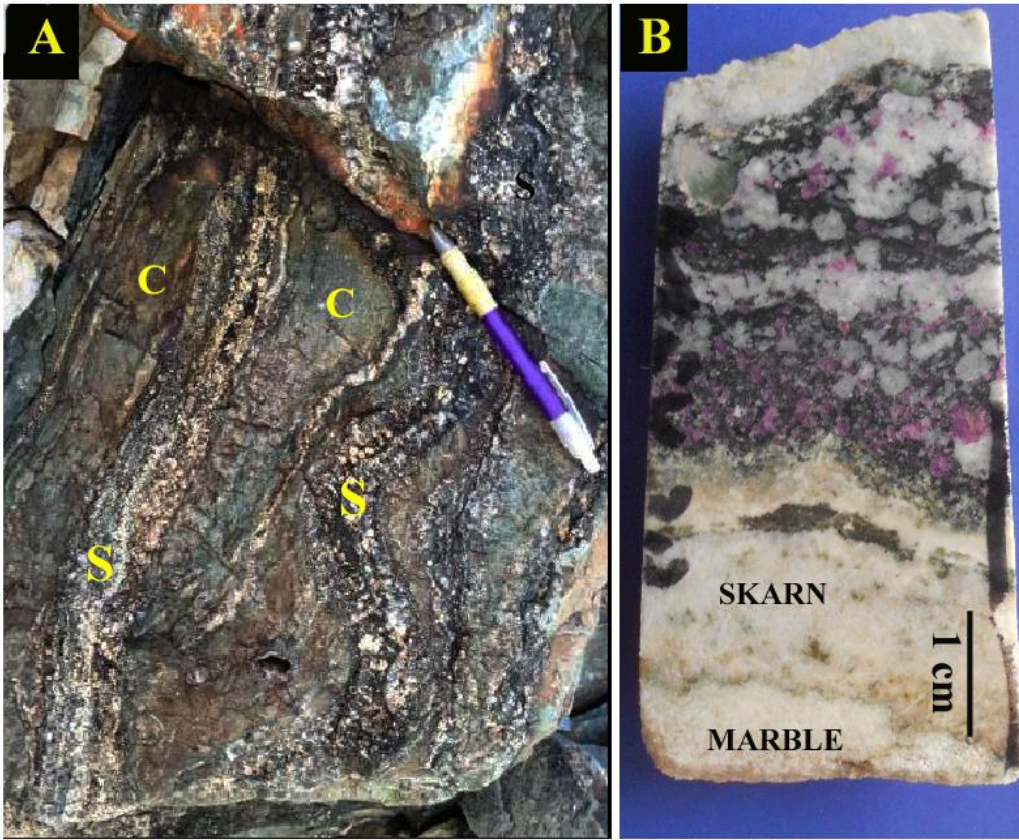


Figure 3. (A) Anastomosing eudialyte veins and skarns (S) with intercalated country rock calcite marble (CC) ; (B) typical eudialyte vein, associated skarn and contact marble.



Prep

Figure 4. Photomicrograph of a scanned thin section in crossed polarized light of the eudialyte vein and skarn illustrated in figure 3 and the mineralogical zones (1-6) investigated in this work. EGM = eudialyte.

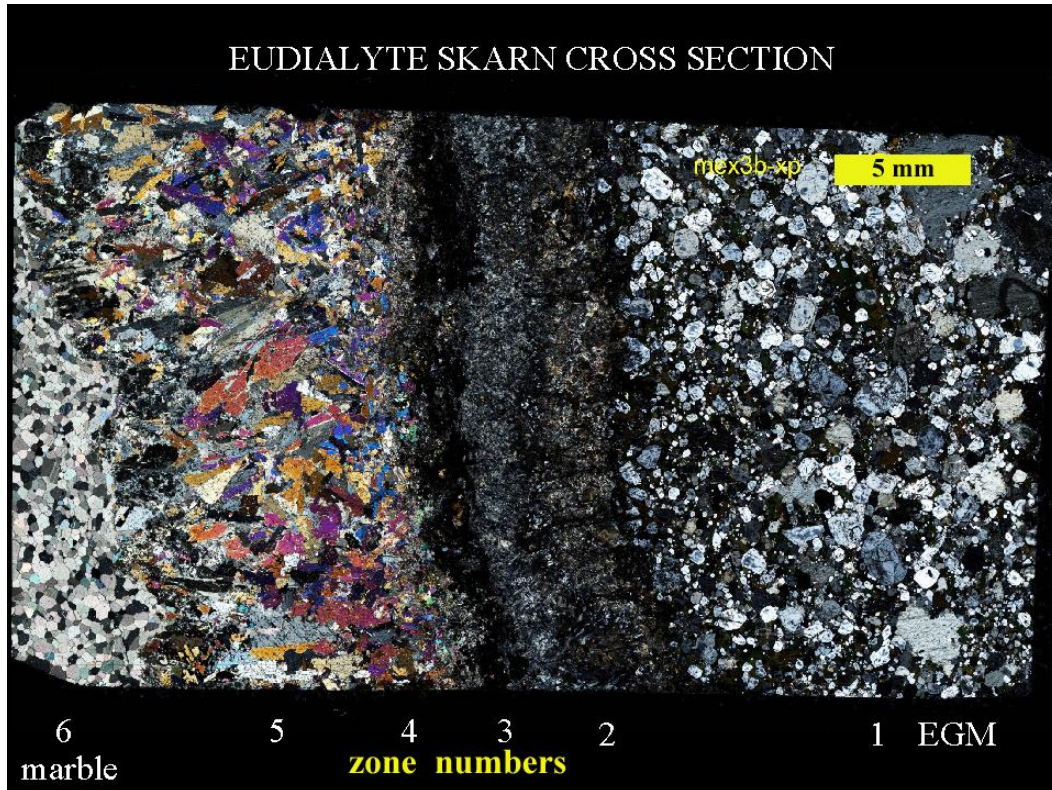


Figure 5. Zone 1 vein with subhedral colourless phenocrysts of eudialyte (EGM) set a matrix of green aegirine (cpx) ; (A) plane polarised light; (B) crossed polars.

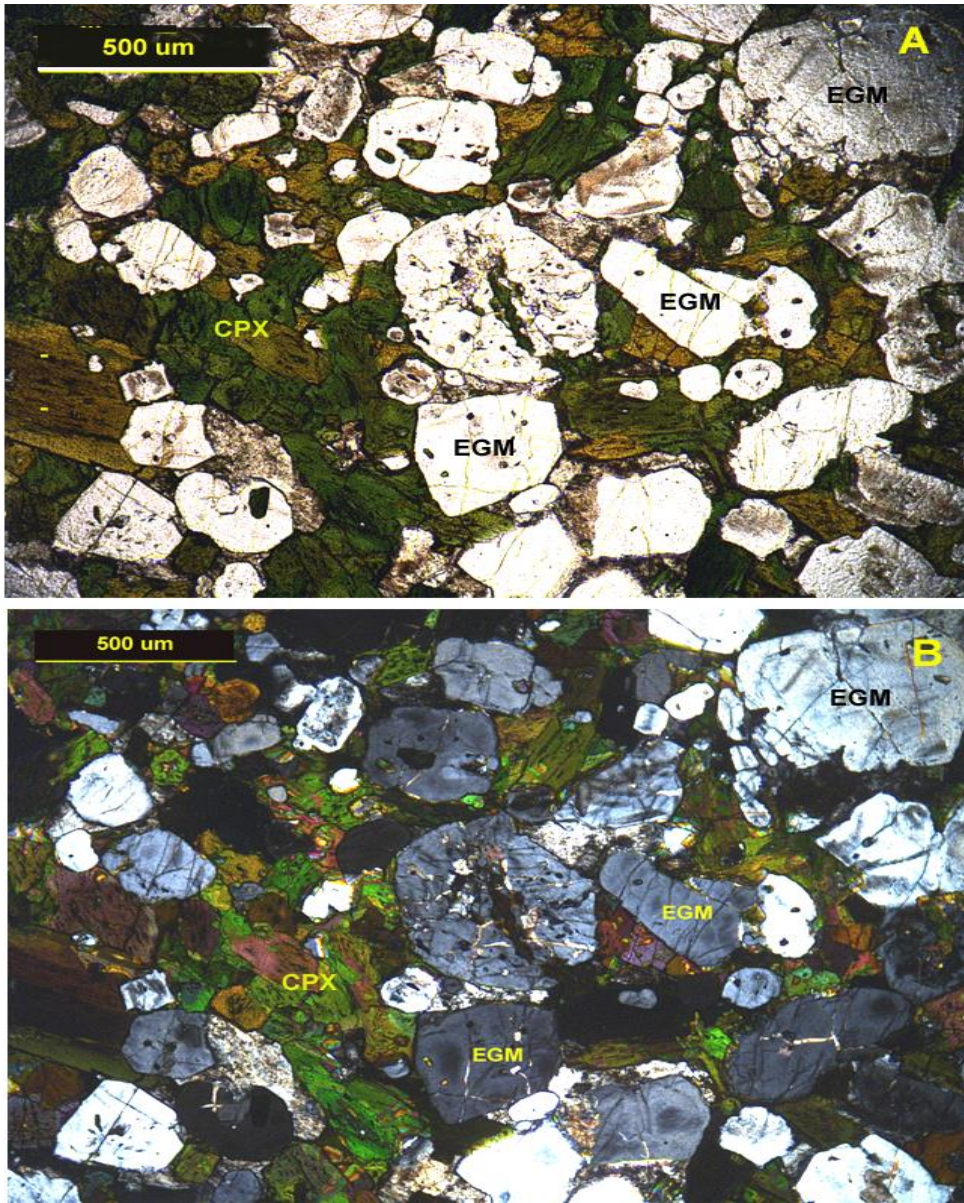


Figure 6. Groundmass of the eudialyte vein. (A) heterogeneous intergrowth of albite and potassium feldspar (K-spar). (B) poikilitic britholite. EGM = eudialyte (back-scattered electron images)

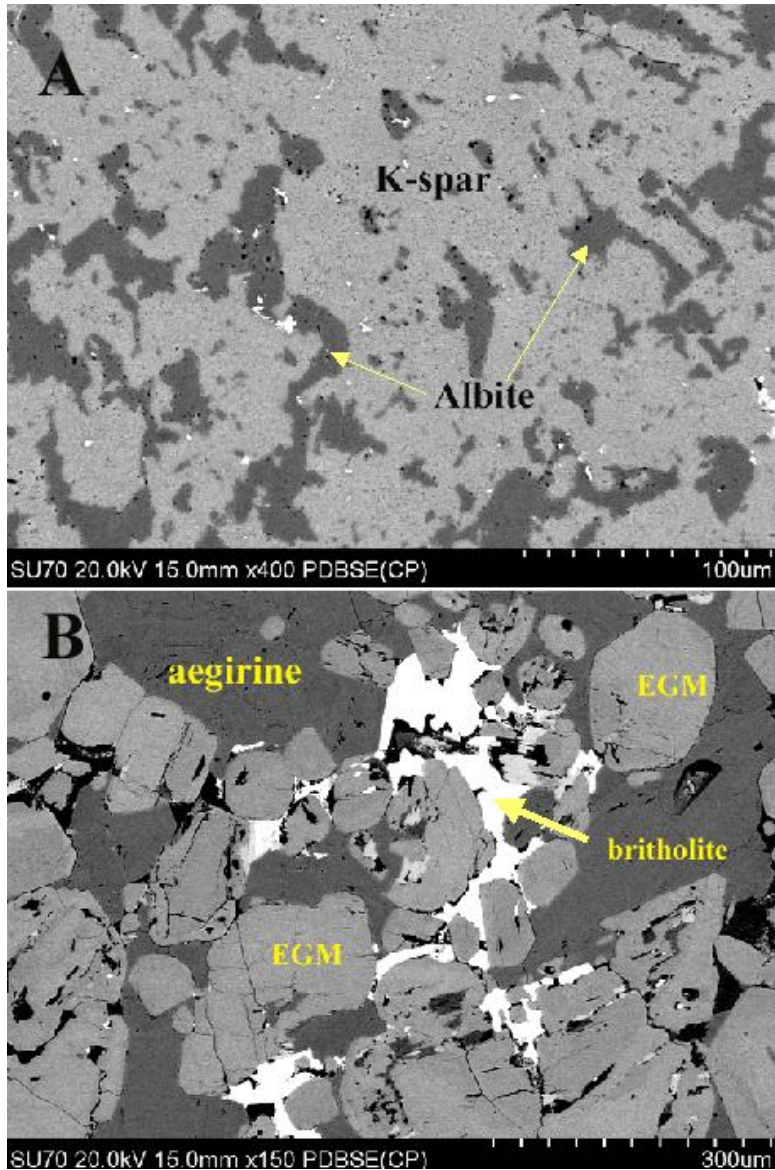


Figure 7. (A) Transition from zone 1 with unaltered eudialyte (EGM) to zone 2 with pseudomorphed eudialyte (ps-EGM). (B) Pseudomorphed eudialyte with cuspidine (csp), wollastonite (Wo), britholite (white), and diopside (cpx). (back-scattered electron images)

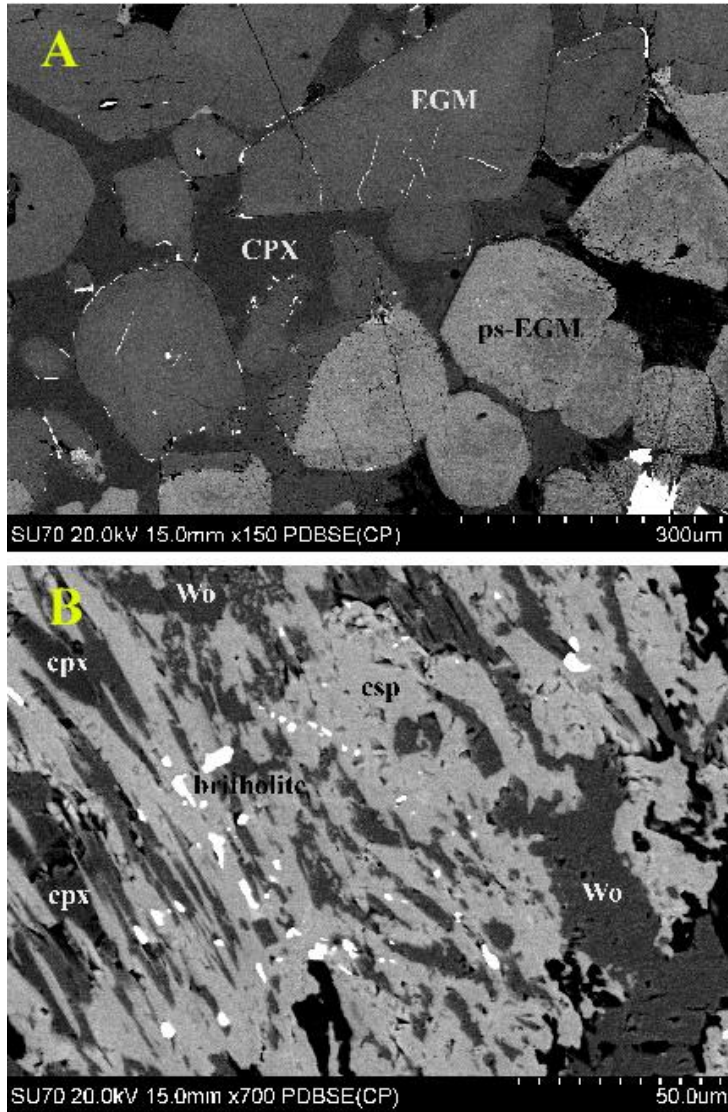


Figure 8. Garnet-bearing Zone 3. (A) Anhedral Zr-bearing andradite and prismatic Zr-bearing

cuspidine set in a wollastonite (Wo) and calcite matrix. The cuspidine prisms are altered at their margins to pectolite. ((B) Zr-bearing andradite with inclusions of Zr-bearing cuspidine (csd) and britholite (white). (back-scattered electron images).

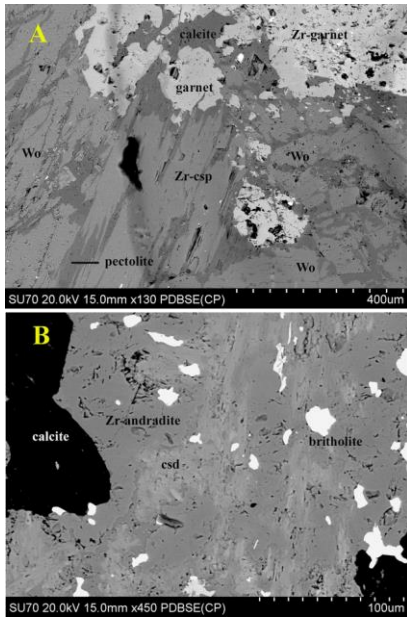


Figure 9. Transition from Zone 4 to the contact marble of zone 6 . (A) Skeletal prisms of cuspidine at the contact with garnet zone 3. (B) Zone 5 Complex intergrowth of plates of

wollastonite (Wo) with prismatic cuspidinehiortdahlite (c-h). (C) Zone 5 prismatic cuspidine-hiortdahlite set in a wollastonite matrix. (D) Contact of zone 5 with the country rock marble (zone 6). The skarn at the contact consists of wollastonite and prisms of cuspidine-hiortdahlite with minor complex intergrowths of diopside, fluorite, apatite and calcite (not shown). (Crossed polarized light images).

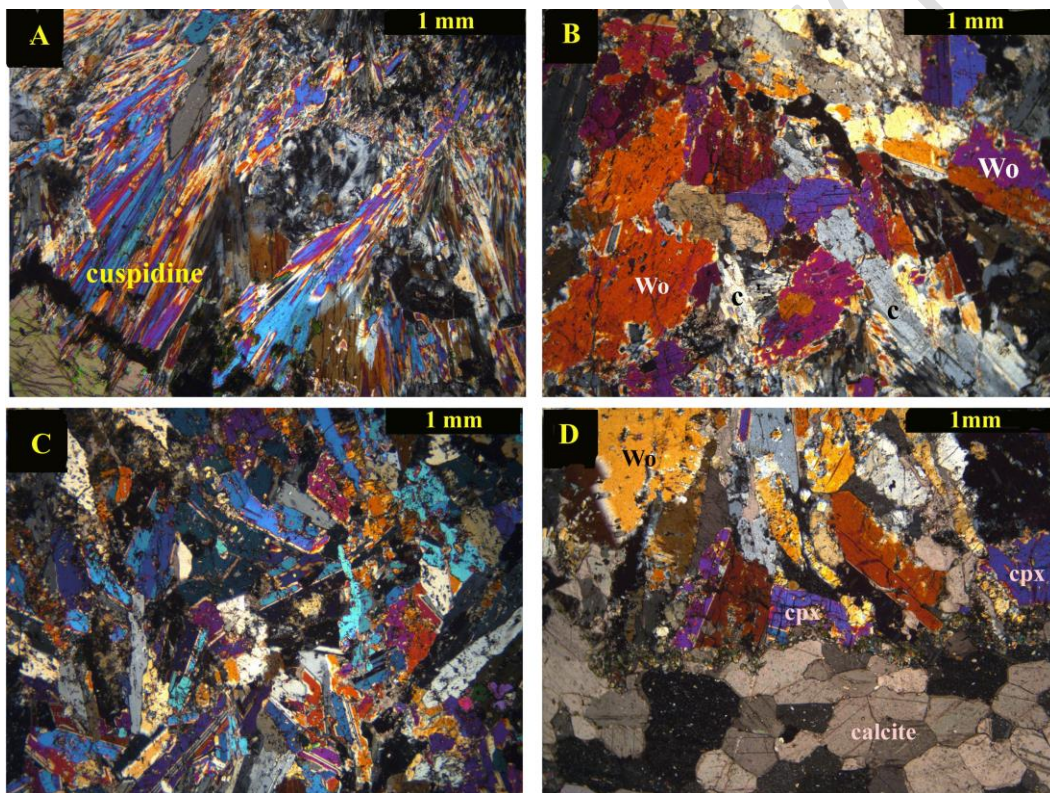


Figure 10. Contact of zone 5 with the marble characterized by long prismatic zoned and resorbed Zr-bearing cuspidine - hiortdahlite solid solutions. (A) Cuspidine prisms (csd) with

diopside (cpx) set in a wollastonite and calcite matrix (cc) (crossed polarised light) (B) Resorbed cuspidine prism showing heterogeneous composition zoning. Regions of higher back-scattered electron contrast are enriched in Zr.

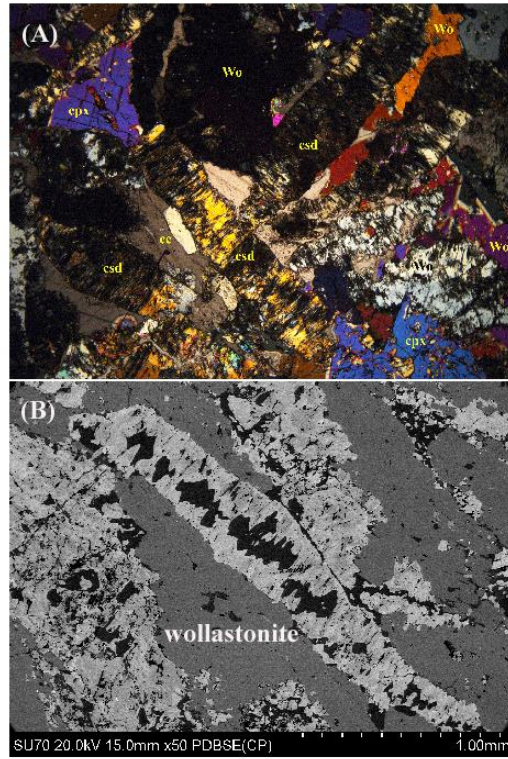


Figure 11. Compositions of Sierra La Vasca (yellow box) eudialyte compared with those of world-wide eudialyte group minerals (after Schilling *et al.* 2011) .

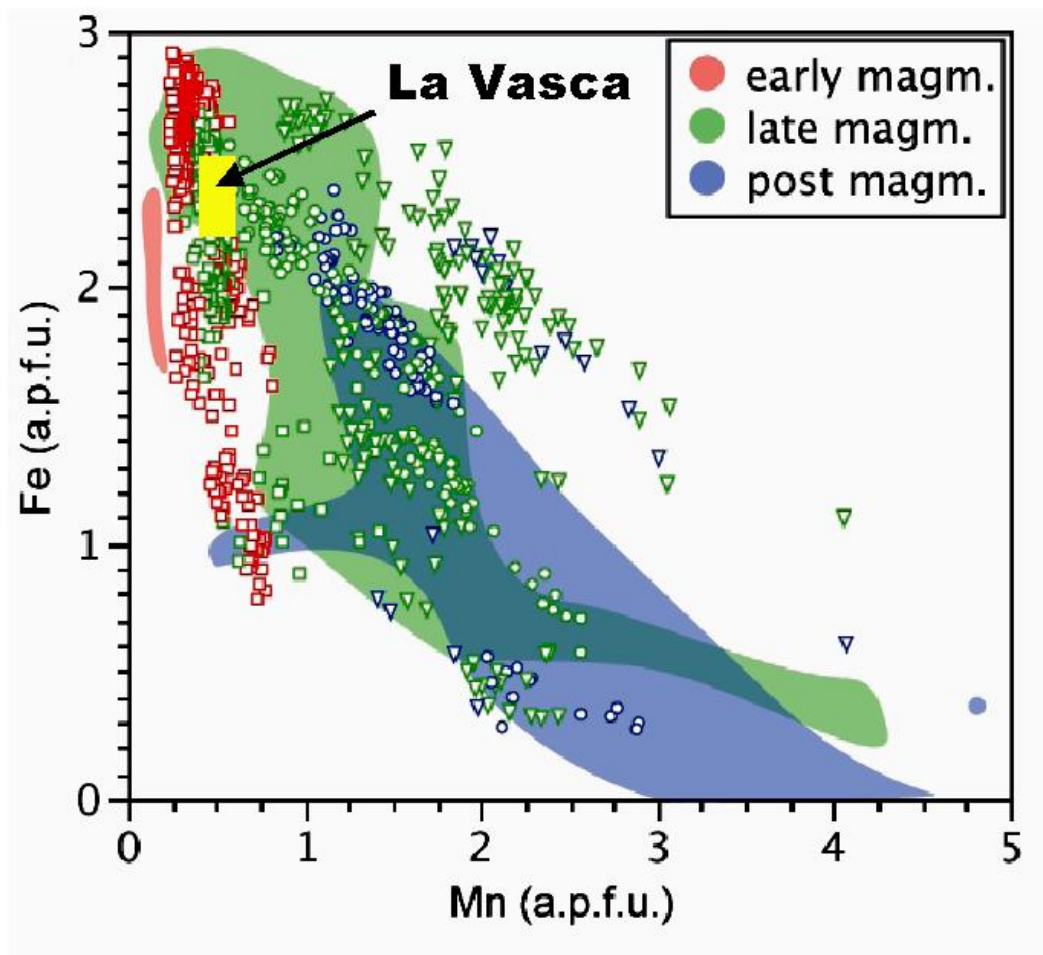


Figure 12. Compositions (apfu) of cuspidine, Zr-bearing cuspidine (c-h) and hiortdahlite from the Sierra La Vasca skarn in the ternary system Ca-Na-Zr (apfu).

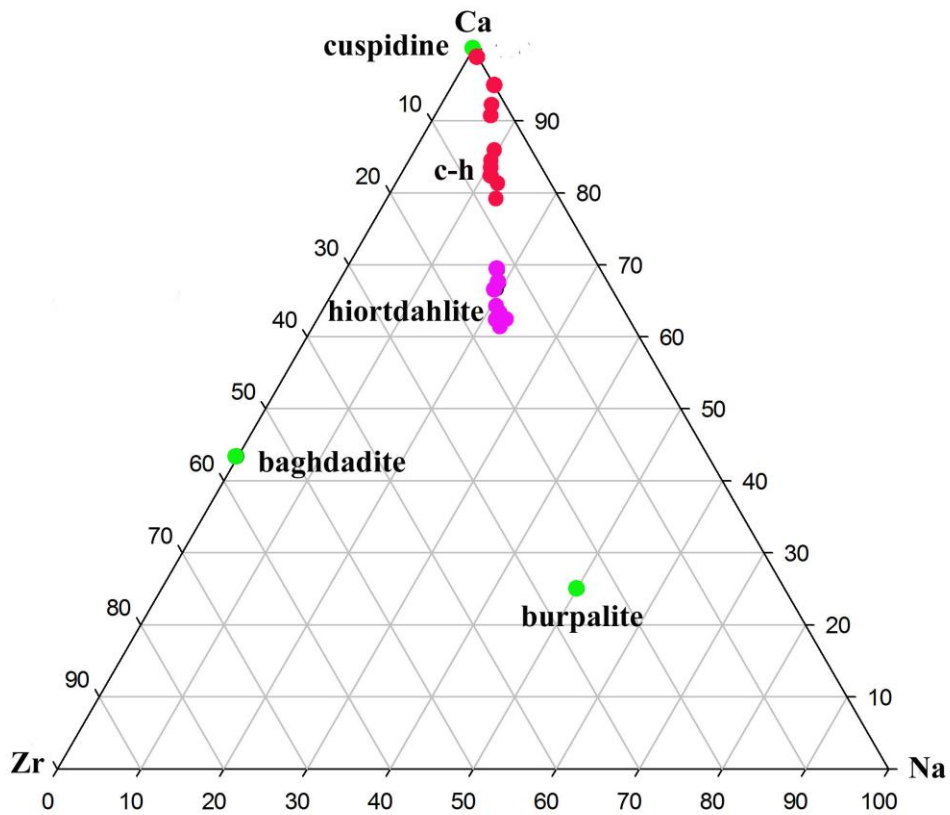


Figure 13. Relative mobility of some elements in the La Vasca skarn,

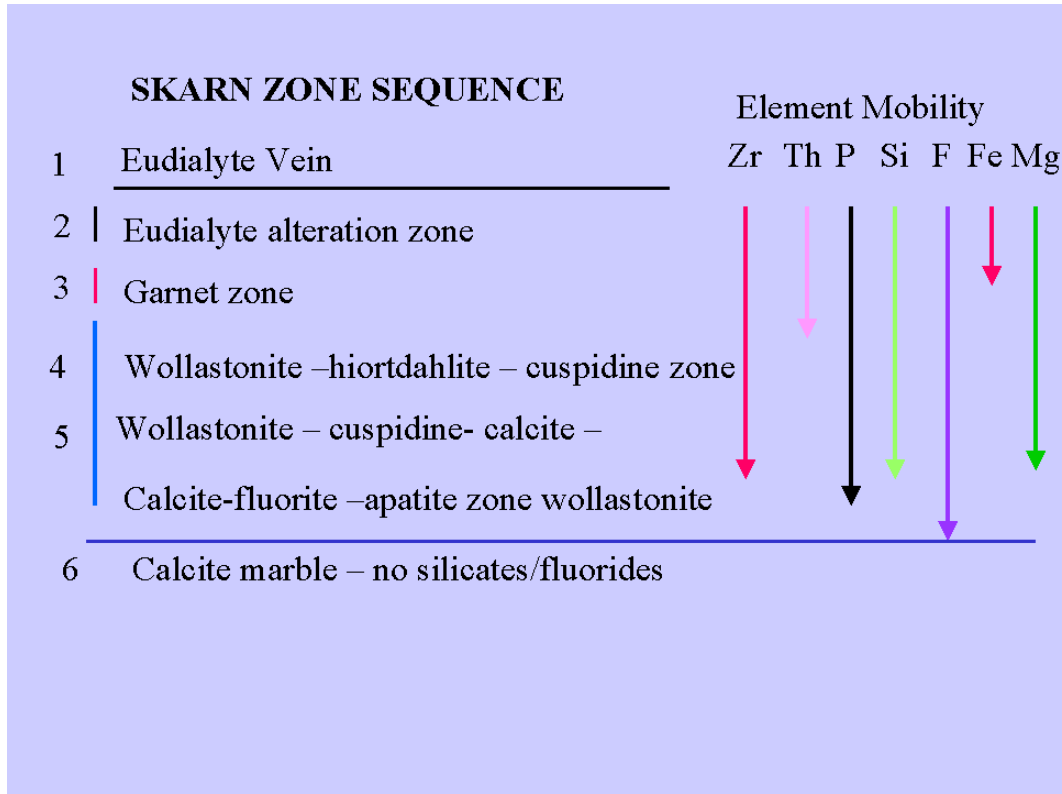


Table 1. Representative compositions of eudialyte.

Wt.%	1	2	3	4	5
Nb ₂ O ₅	n.d.	n.d.	n.d.	n.d.	0.84
ZrO ₂	10.59	11.06	10.42	10.02	10.30
SiO ₂	50.87	51.82	50.96	50.21	49.75
TiO ₂	0.20	0.35	0.51	0.57	0.67
La ₂ O ₃	0.34	0.19	0.26	0.28	0.45
Ce ₂ O ₃	0.86	0.63	0.58	0.60	0.77
Nd ₂ O ₃	0.40	0.54	0.32	0.37	0.56
MnO	1.26	0.91	0.99	0.98	1.23
FeO	5.20	5.52	5.33	5.64	5.37
CaO	11.91	11.77	11.70	11.77	11.83

Na ₂ O	12.46	12.57	13.14	13.40	12.61
K ₂ O	0.33	0.44	0.37	0.22	0.24
Cl	2.38	2.46	2.34	2.38	2.41
Sum	96.80	98.26	96.92	96.44	97.03
O=Cl	0.54	0.56	0.53	0.54	0.54
Total	96.26	97.70	96.39	05.90	96.49
Cations					
Nb					0.198
Zr	2.665	2.721	2.611	2.552	2.617
Si	26.257	26.146	26,191	26.224	25.923
Ti	0.078	0.133	0.197	0.224	0.263
La	0.065	0.035	0.049	0.054	0.086
Ce	0.163	0.117	0.109	0.115	0.147
Nd	0.074	0.097	0.059	0.069	0.104
Mn	0.551	0.389	0.431	0.434	0.543
Fe	2.245	2.329	2.291	2.463	2.340
Ca	6.587	6.363	6.443	5.586	6.604
Na	12.469	12.297	13.094	13.569	12.739
K	0.217	0.283	0.243	0.147	0.159
Cl	2.082	2.104	2.038	2.107	2.128
Cation Sum	51.370	50.910	51.719	52.437	51.724
End Members					
Eud	75	78	76	82	78
Kb	18	13	14	14	18
Allu	7	9	9	3	4

Eud = eudialyte; Kb = kentbrooksit; Allu = alluaivite. End members calculated after Pfaff *et al.* (2010)

Table 2. Representative compositions of hiortdahlite and wöhlerite.

wt.%	1	2	3	4	5	6	7	8	9
F	7.91	7.99	7.40	7.43	7.29	7.25	4.78	3.25	8.41
Na ₂ O	5.90	5.66	5.95	6.51	6.64	6.88	7.07	7.22	6.62
SiO ₂	29.83	29.99	29.65	29.96	29.73	29.98	30.69	30.04	30.76
CaO	37.24	38.93	36.79	34.81	34.83	33.95	30.63	28.74	32.90
TiO ₂	0.57	0.59	0.97	0.65	0.50	0.73	2.10	0.21	0.98
MnO	0.18	0.27	0.32	0.24	0.05	0.24	0.46	0.26	0.92
FeO	0.24	0.30	0.22	0.42	0.33	0.20	0.73	0.31	1.17
ZrO ₂	15.91	15.26	16.51	18.24	19.73	19.49	13.51	15.56	17.12
Nb ₂ O ₅	1.36	0.99	1.39	0.93	0.84	1.09	10.01	13.75	1.90
	99.14	99.98	99.20	99.19	99.94	99.81	99.98	99.34	100.78
O=F	3.33	3.36	3.11	3.13	3.07	3.05	2.01	1.37	2.78
Total	95.81	96.62	96.09	96.06	96.87	96.76	97.97	97.97	98.00
S.F									
F	6.619	6.631	6.192	6.236	6.094	6.061	3.965	2.805	6.894
Na	3.027	2.880	3.052	3.350	3.403	3.527	3.595	3.520	3.327
Si	7.893	7.870	7.844	7.951	7.859	7.925	8.049	7.843	7.973
Ca	10.558	10.947	10.429	9.899	9.865	9.617	8.608	8.403	9.138
Ti	0.113	0.116	0.193	0.130	0.119	0.145	0.464	0.043	0.191
Mn	0.040	0.060	0.072	0.054	0.020	0.054	0.102	0.060	0.202
Fe	0.053	0.066	0.049	0.093	0.073	0.044	0.160	0.071	0.254
Zr	2.053	1.953	2.169	2.360	2.543	2.513	1.728	2.071	2.164
Nb	0.163	0.118	0.166	0.112	0.100	0.130	1.187	1.696	0.227
∑X	16.01	16.14	16.13	15.99	16.12	16.03	15.79	16.16	15.56
∑Cat	23.90	24.01	23.98	23.95	23.98	23.95	24.01	23.80	23.53

S.F. = Structural formulae calculated for 36 atoms of oxygen. Compositions: 1-3 hiortdahlite replacing eudialyte; 4-6 hiortdahlite in skarn zone 3; 7-8 wöhlerite in skarn zone; 9 hiortdahlite from the type locality, Langodden, Norway (Dal Bo *et al.*2022)

Table 3. Representative compositions of cuspidine and cuspidine-hiortdahlite solid solutions

wt.%	1	2	3	4	5	6	7	8
F	10.69	11.41	10.74	8.94	9.43	9.42	9.19	8.72
Na	n.d.	0.37	1.64	2.98	3.12	3.27	4.41	4.11
Si	31.51	31.75	32.02	31.81	31.68	31.91	31.58	31.62
Ca	59.20	57.76	55.87	48.24	48.09	47.61	46.79	44.79
Zr	n.d.	n.d.	n.d.	6.06	6.99	7.64	8.41	9.50
Sum	101.40	101.29	100.27	98.03	99.31	99.85	100.38	98.74
O=F	4.50	4.80	4.52	3.76	3.97	3.97	3.87	3.67
Total	96.90	96.49	95.75	94.27	95.34	95.88	96.51	95.07
S.F.								
F	8.490	9.035	8.582	7.663	7.689	7.642	7.509	7.180
Na	-	-	0.804	1.505	1.560	1.626	1.708	2.075
Si	7.928	7.949	8.091	8.284	8.167	8.185	8.159	8.233
Ca	15.924	15.495	15.126	13.460	13.284	13.085	12.453	12.495
Zr	-	-	-	0.700	0.879	0.956	1.060	1.206
ΣX	15.92	15.68	15.93	15.73	15.42	15.67	15.72	15.78
ΣCat	23.84	23.62	24.02	24.02	23.89	23.85	23.88	24.01

S.F. = structural formula based on 36 (O,F). Compositions: 1-3 cuspidine; 4-8 cuspidine-hiortdahlite solid solutions.

Table 4. Representative compositions of diopside (Cpx) and Ca-catapleiite (Catapl).

Wt.%	Cpx-1	Cpx-2	Cpx-3	Catapl-1	Catapl-2	Catapl-3
SiO ₂	53.79	54.97	54.34	43.29	42.90	43.51
ZrO ₂	n.a.	n.a.	n.a.	28.60	28.27	27.15
Al ₂ O ₃	0.30	n.d.	n.d.	n.d.	n.d.	n.d.
FeO _T	2.18	3.07	3.15	0.41	0.29	0.30
MnO	0.47	1.08	0.83	n.d.	n.d.	n.d.
MgO	16.82	15.86	16.32	n.d.	n.d.	n.d.
CaO	25.68	25.60	25.68	13.67	13.34	13.35
Na ₂ O	0.18	0.16	0.23	0.62	0.80	0.91

Sum	99.42	100.58	100.55	-	-	-
FeO calc	0.13	2.83	1.08	-	-	-
Fe ₂ O ₃ calc	2.28	0.27	2.30	-	-	-
Total	99.65	100.77	100.78	86.58	85.59	85.22
SF	4/6	4/6	4/6	9	9	9
Si	1.969	2.002	1.977	2.996	3.004	3.037
Zr	-	-	-	0.965	0.964	0.934
Al	0.013	-	-	-	-	-
Fe ²⁺	0.004	0.086	0.033	0.024	0.017	0.018
Fe ³⁺	0.063	0.007	0.063	-	-	-
Mn	0.015	0.033	0.026	-	-	-
Mg	0.918	0.861	0.885	-	-	-
Ca	1.007	0.999	1.001	1.014	1.000	0.998
Na	0.013	0.011	0.016	0.083	0.109	0.123
Total	4.002	3.999	4.001	5.032	5.094	5.100

SF = structural formula calculated on 4 cations and 6 oxygens for diopside and 9 oxygens for calcium catapleite. Fe²⁺ and Fe³⁺ for diopside calculated following Droop (1987).
n.d. = not detected; n.a. = not analysed

Table 5. Representative compositions of britholite

Wt.%	1	2	3	4	5
SiO ₂	21.28	20.72	19.42	19.93	17.76
P ₂ O ₅	0.86	1.46	3.03	3.94	6.06
CaO	13.96	14.76	16.80	17.98	19.75
Y ₂ O ₃	5.92	3.34	3.09	1.43	2.20
La ₂ O ₃	7.64	9.38	10.24	10.81	10.28
Ce ₂ O ₃	21.10	24.84	23.21	25.60	22.72
Pr ₂ O ₃	2.77	3.07	2.66	3.17	2.60
Nd ₂ O ₃	11.83	12.53	10.06	10.55	8.97
Sm ₂ O ₃	3.22	2.94	2.14	2.20	1.72
Gd ₂ O ₃	2.85	2.29	1.71	1.52	1.43
Dy ₂ O ₃	1.86	1.27	1.13	0.59	0.73

ThO ₂	0.33	0.26	1.24	1.24	0.34
sum	93.65	96.86	94.73	98.96	94.56
SF	13	13	13	13	13
Si	2.99	2.89	2.67	2.63	2.37
P	0.10	0.16	0.36	0.46	0.68
Ca	2.11	2.21	2.47	2.50	2.83
Y	0.46	0.26	0.23	0.10	0.16
La	0.39	0.49	0.52	0.52	0.52
Ce	1.14	1.27	1.17	1.24	1.11
Pr	0.13	0.16	0.13	0.16	0.13
Nd	0.59	0.61	0.49	0.49	0.42
Sm	0.16	0.13	0.10	0.10	0.07
Gd	0.13	0.09	0.07	0.07	0.07
Dy	0.10	0.07	0.07	0.03	0.03
Th	0.01	0.01	0.03	0.03	0.01
sum	8.31	7.91	8.31	8.50	8.40
A-site	3.09	3.05	3.03	3.09	3.05
B-site	5.22	4.86	5.28	5.41	5.35

Table 6. Representative compositions of garnet

Wt.%	1	2	3
SiO ₂	35.61	35.33	33.55
TiO ₂	0.11	0.09	0.69
Al ₂ O ₃	0.76	0.78	0.96
CaO	32.82	32.14	31.26
MnO	0.56	0.62	0.75
Fe ₂ O ₃	30.34	29.36	29.67
ZrO ₂	n.d.	1.03	3.56
Sum	100.40	99.35	100.44
SF	12	12	12
Si	2.996	3.001	2.857
Al	0.076	0.078	0.096

Ti	0.007	0.005	0.044
Ca	2.959	2.925	2.852
Mn	0.040	0.045	0.044
Fe ³⁺	1.921	1.877	1.901
Zr	-	0.043	0.148
Total	7.989	7.974	7.942

SF = structural formula on the basis of 12 oxygens
Total Fe is expressed as Fe³⁺; n.d. = not detected.

Prepublished article